

# Assessment of the efficiency gains introduced by novel aero engine concepts

ISABE-2013-1720

R. Becker, M. Schaefer, S. Reitenbach  
 German Aerospace Center e.V. - DLR  
 Institute of Propulsion Technology  
 Linder Hoehe, 51147 Cologne, Germany

## Abstract

The purpose of the present study is to investigate fuel efficiency gains introduced by two novel aero engine concepts available in the timeframe of 2025. The analysis focuses on the assessment of geared turbofan (GTF) and counter rotating open rotor (CROR) concepts in regard to their potential to improve global aero engine efficiency. Since the CROR engine is most likely to be integrated into short and medium range aircraft, the airframe application considered in the present investigation is a 150 passenger short range airliner. The efficiency benefits of the engine concepts mentioned above are assessed in two steps. At first, representative models of both concepts are optimized for a set of discrete operating points, which stem from the baseline top level aircraft requirements. To preserve comparability between the novel concepts, component efficiencies and cooling technology of the core engines are aligned to a common technology level while taking into account concept-specific characteristics. Engine weight and drag estimations are performed on the basis of conceptual annulus designs. The operating point based optimization results are presented and compared to a baseline engine. In step two, installation effects are accounted for, as the engines are installed to the airframe model and analyzed on flight mission level.

## Nomenclature

|      |                             |
|------|-----------------------------|
| BPR  | bypass ratio                |
| CR   | cruise condition            |
| CROR | counter rotating open rotor |
| EOF  | end of field condition      |
| FPR  | fan pressure ratio          |
| FN   | net thrust                  |
| GTF  | geared turbofan             |
| HPC  | high pressure compressor    |
| HPT  | high pressure turbine       |
| LPC  | low pressure compressor     |
| LPT  | low pressure turbine        |
| OPR  | overall pressure ratio      |
| PWX  | power extraction            |
| SFC  | specific fuel consumption   |
| SLS  | sea level static            |
| TET  | turbine entry temperature   |
| TOC  | top of climb                |

## Introduction

The goals defined by the ACARE Vision 2020 - to reduce aircraft fuel consumption by 50%, NO<sub>x</sub> production by 80% and to half current perceived noise levels - still present a major challenge to aerospace industry. Soaring fuel prices and intensified concerns about climate change increase the pressure on engine manufacturers to offer novel aero engines that provide substantial fuel efficiency improvements.

Basically, aero engine efficiency can be increased by the improvement of two fundamental parameters, namely thermal and propulsive efficiency. For conventional gas turbine cycles the thermal efficiency depends on OPR,

temperature ratio as well as component efficiencies and cooling technology. The potential to substantially improve the thermal efficiency of conventional cycle engines is limited because the technology of the driving factors is already on a mature level [1]. While heat exchanged cycles like e.g. intercooled recuperated turbofans address the improvement of thermal efficiency, their deployment is unsettled since heat exchanger pressure losses and effectiveness as well as weight penalties still present major challenges to engineers [2]. Therefore the only way to significantly reduce fuel burn in a medium term perspective is to increase propulsive efficiency, which is mainly addressed by reducing the engine's specific thrust and increasing bypass ratio.

Two promising candidate concepts in terms of further increasing propulsive efficiency are the geared turbofan and notably the counter rotating open rotor. The advanced conventional turbofan drops behind because of its assumed limited potential to significantly increase the bypass ratio and thus propulsive efficiency as described in reference [3]. For the present assessment three engine models are evaluated and designed to power a short-haul civil airliner. A conventional turbofan engine comparable to engine technology currently in use is considered as the baseline engine. In the following, two more engine models are presented: An advanced GTF with a takeoff bypass ratio of approximately 14 as well as a geared CROR engine. The performance models are designed to re-engine the baseline airliner. All engines are modeled by means of DLR's in-house gas turbine performance code GTlab [4]. For investigations on flight mission level, DLR's aircraft performance tool VarMission is used [5], which is coupled to the GTlab engine simulation software. To optimize the engine cycles the multidisciplinary design

optimization software ModelCenter™ [6] is employed.

### Engine requirements

The top level engine requirements stem from the assumed airframe and flight mission scenario. For the present study a generic 150pax aircraft configuration similar to the A320 was chosen. Table 1 summarizes the assumed aircraft specifications.

| <i>Parameter</i> | <i>Unit</i> | <i>Value</i> |
|------------------|-------------|--------------|
| Number PAX       | [-]         | 150          |
| Design range     | [km]        | 4465         |
| CR Altitude      | [ft]        | 35000        |
| CR speed         | [Mach]      | 0.78         |
| TOFL             | [m]         | 2000         |
| MTOW             | [kg]        | 77000        |

**Table 1: Top level aircraft specifications**

Three aircraft operating points were considered in order to generate the conceptual designs for the CROR and GTF engine respectively. The aerodynamic design point for both engines is the cruise condition (CR). Additionally, two off-design points were evaluated to satisfy the most important design requirements: The end of field condition (EOF) exerts the highest thermal and mechanical loads on the engine, which practically sizes the cooling flow requirements. At the top of climb (TOC) operating point, maximum corrected speeds and corrected mass flows are encountered. Table 2 lists the mission point description and thrust requirements of the aircraft model used for this study.

| <i>Parameter</i> | <i>Unit</i> | <i>CR</i> | <i>TOC</i> | <i>EOF</i> |
|------------------|-------------|-----------|------------|------------|
| Altitude         | [m]         | 10668     | 10668      | 0          |
| Mach No.         | [-]         | 0.78      | 0.78       | 0.2        |
| $\Delta T_{ISA}$ | [K]         | 10        | 10         | 15         |
| FN               | [kN]        | 21.1      | 23.7       | 92.5       |
| HP-PWX           | [kW]        | 142.5     | 142.5      | 127.5      |

**Table 2: Mission design point requirements**

Furthermore, the aircraft power requirements are shown in table 2,

which are assumed to be supplied as electrical power only.

### **Baseline Engine**

A two-shaft mixed flow turbofan engine similar to the IAE-V2500-A5 was chosen as baseline. The engine performance model was aligned with figures taken from emission certification [7] and validated against control unit data recorded at pass-off tests during a shop visit of DLR's in-house experimental A320 aircraft. A more detailed description of the validation process and the resulting performance model can be found in [8].

### **Engine Design methodology**

At the beginning of the design process, predetermined principal engine layouts for both novel concepts were assumed. The GTF engine was set up as a standard two shaft geared turbofan. For the CROR an aft mounted three shaft pusher configuration was chosen. Here, a two-shaft core engine drives a free power turbine which is connected to the propellers via a planetary differential gearbox. Both novel engine concepts were numerically optimized on basis of the three aircraft operating point requirements given above. The cruise condition was selected as the master design point since it is the most important flight condition in terms of fuel burn. The remaining operating conditions provided off-design data that had to be checked against engine requirements and technological constraints. In order to capture the influence of engine installation on the fuel efficiency of the overall aircraft, weight and drag estimations of the propulsion system were conducted. Differences between weight and drag of the baseline engine and the estimation results were used to adjust the aircrafts thrust requirements at the considered mission points. Drag adjustments were carried out as

modifications to the zero-lift drag coefficient of the corresponding aircraft polar. Estimated weight deltas simply add up to the aircraft total weight. In consequence to the thrust adjustments fuel flow at cruise condition was considered as the figure of merit. For each concept a set of independent design variables was modified by the optimizer in order to find the optimum solution in terms of cruise fuel efficiency. Table 3 provides the cruise design parameters and their corresponding design ranges for both engine concepts.

| <i>Concept</i> | <i>Parameter</i> | <i>Unit</i> | <i>Min</i> | <i>Max</i> |
|----------------|------------------|-------------|------------|------------|
| GTF            | LPC PR           | [-]         | 2.0        | 5.0        |
|                | HPC PR           | [-]         | 5.0        | 15.0       |
|                | TET              | [K]         | 1500       | 1600       |
|                | BPR              | [-]         | 10         | 16         |
| CROR           | LPC PR           | [-]         | 5.0        | 10         |
|                | HPC PR           | [-]         | 5.0        | 10         |
|                | TET              | [K]         | 1550       | 1650       |

**Table 3: Independent design parameters for the automated optimization process**

In case of the geared turbofan, the fan pressure ratio was automatically iterated to achieve an optimal velocity ratio between core and bypass nozzle. Additionally a variable area bypass nozzle was assumed to guarantee sufficient fan stall margin at all flight conditions. The open rotor model utilizes a constant speed propeller configuration as described in [9]. Component design-efficiencies for core engine compressors and turbines of all engine setups were defined using correlation methods from [10]. Besides the requirements and design parameters several technological constraints were considered as listed in Table 4. Maximum temperature levels were chosen to be slightly lower than the maximum temperature capabilities considered in previous studies e.g. [11] and [12], which are intended to reflect short range specific characteristics in respect to hot end life use due

to the large number of flight cycles.

| <i>Parameter</i>       | <i>Unit</i>                       | <i>Limit</i>         |
|------------------------|-----------------------------------|----------------------|
| Max T3@EOF             | [K]                               | 930 K                |
| Max T4@EOF             | [K]                               | 1820 K               |
| Max T <sub>metal</sub> | [K]                               | 1220 K               |
| Min HPC Bld. Height    | [mm]                              | 13.5 mm              |
| Max AN <sup>2</sup>    | [m <sup>2</sup> /s <sup>2</sup> ] | 1.35x10 <sup>4</sup> |

**Table 4: Assumed technological constraints**

A minimum blade height constraint of 13.5 mm for the last stage of the high pressure compressors was introduced to avoid exceedingly high tip clearance losses. Cooling air requirements at EOF were computed with the semi empirical method proposed by Horlock et al [13]. Therein film cooling was considered for all vanes and blades of the cooled turbines. Maximum average metal temperatures of the turbine blades were set to 1220K, the film cooling effectiveness was assumed to be 0.7. Additionally the maximum AN<sup>2</sup> of the high speed low pressure turbines was restricted.

### **Geometry, weight and drag estimation**

The weight and drag estimation methodology of the current study is based on the results of a conceptual flow path design process. Taking the result data of the underlying thermodynamic cycle into account, annulus designs for the turbo components and the combustors were performed. The main input parameters for the annulus calculations are the axial inlet and outlet Mach numbers of the components as well as the stations' hub-to-tip ratios. The values of both parameter sets were kept constant during the optimization process. In case of compressors and turbines, average stage loading and aspect ratio distributions have been applied as additional input factors. Constant compressor and propulsor tip speeds were used to set the shaft speeds which allowed for loading calculations of all other turbo components. The resulting component

annulus approximations were assembled to an overall bare engine flow path which provided the input parameters for the subsequent components weight and nacelle geometry calculations. Weight estimations for the standard jet engine components were performed by use of the statistical method presented by Sagerser et al [14]. Thereby all necessary geometry and speed information was taken from the annulus computation presented above. Correlation factors proposed by Sagerser have been maintained except for the structure weight correlation coefficient, which was adjusted to 0.35 to compensate the known under ratings of the method [15]. Since gearbox and propeller weight calculations are not included in investigations of Sagerser, different procedures have been applied. Gearbox weight estimation was performed by use of the correlation given in [16]. Open rotor propeller weight estimation was based on empirical data published in [17]. Besides the weight calculations, nacelle drag was estimated for all considered engines by means of the component build up methodology proposed by Raymer [18]. Zero-lift drag coefficient was computed from equation (1)

$$C_{d,0} = \frac{C_f \cdot FF \cdot IF \cdot S_{wet}}{S_{ref}} \quad (1)$$

The aircrafts wing area  $S_{ref}$  equals 122.4 m<sup>2</sup>, interference factor IF was set to 1.3 for all engines. The form factor was computed by equation (2)

$$FF = 1 + \left( \frac{0,35d}{l} \right) \quad (2)$$

For the novel engine concepts the maximum nacelle diameter  $d$ , overall nacelle length  $l$  and wetted area  $S_{wet}$  stem from the nacelle geometry computations. The baseline engines geometry data was extracted from CAD data provided as described in [8]. The flat-plate skin friction

coefficient for turbulent flow was determined by equation (3)

$$C_f = \frac{0,455}{(\log_{10} R)^{2,58} \cdot (1 + 0,144M^2)^{0,65}} \quad (3)$$

Finally the resulting deltas between the computed zero-lift coefficients for the novel concepts and the V2500 reference engine have been used as corrections to the aircraft's Mach-number-dependent lift-to-drag characteristics, to account for engine installation.

### **Optimization results and uninstalled performance assessment**

Table 5 lists the main results of the optimization process.

| <b>Component</b>         | <b>Parameter</b> | <b>Unit</b>            | <b>GTF</b>   | <b>CROR</b>  |
|--------------------------|------------------|------------------------|--------------|--------------|
| <b>LPC / Booster</b>     | PR               | [-]                    | 3.02         | 5.57         |
|                          | Stages           | [-]                    | 4            | 5            |
|                          | $\eta_{is}$      | [-]                    | 0.907        | 0.899        |
| <b>HPC</b>               | PR               | [-]                    | 11.4         | 7.9          |
|                          | Stages           | [-]                    | 8            | 5            |
|                          | $\eta_{is}$      | [-]                    | 0.891        | 0.896        |
| <b>HPT</b>               | Stages           | [-]                    | 2            | 1            |
|                          | $\eta_{is}$      | [-]                    | 0.897        | 0.893        |
| <b>IPT</b>               | Stages           | [-]                    | n/a          | 1            |
|                          | $\eta_{is}$      | [-]                    | n/a          | 0.898        |
| <b>LPT</b>               | Stages           | [-]                    | 3            | 3            |
|                          | $\eta_{is}$      | [-]                    | 0.94         | 0.94         |
| <b>Propeller or Fan</b>  | <b>Diameter</b>  | <b>[m]</b>             | <b>2.06</b>  | <b>4.27</b>  |
|                          | PR               | [-]                    | <b>1.383</b> | <b>n/a</b>   |
|                          | $\eta$ (CR)      | [-]                    | <b>0.921</b> | <b>0.853</b> |
| <b>Overall Parameter</b> |                  | <b>Unit</b>            | <b>GTF</b>   | <b>CROR</b>  |
| OPR                      |                  | [-]                    | <b>46.98</b> | <b>43.43</b> |
| BPR                      |                  | [-]                    | <b>12.2</b>  | <b>~90</b>   |
| TSFC                     |                  | <b>[g/kNs]</b>         | <b>13.67</b> | <b>12.11</b> |
| Gear Ratio               |                  | [-]                    | <b>3.1</b>   | <b>9.5</b>   |
| Bare Engine Length       |                  | <b>[m]</b>             | <b>3.36</b>  | <b>4.42</b>  |
| Nacelle Wetted Area      |                  | <b>[m<sup>2</sup>]</b> | <b>31.1</b>  | <b>19.3</b>  |
| Engine POD Weight        |                  | <b>[kg]</b>            | <b>3201</b>  | <b>4097</b>  |

**Table 5: Optimization results for GTF and CROR. Performance parameters are given for cruise conditions.**

The final GTF configuration features a 12.2 cruise bypass ratio which leads to a fan diameter of approximately 2.06 meters. The ideal fan pressure ratio was found to be 1.38. The fan is connected via a gearbox of transmission ratio 3.1 to

a three stage high speed low pressure turbine (LPT). The GTF core is comprised of a four stage booster, which is directly connected to the LPT, as well as an eight stage high pressure compressor (HPC) driven by a two stage high pressure turbine (HPT). An overall weight of the GTF propulsion system of 3201kg is predicted, which is approximately 200kg below the weight of the V2500-A5 propulsion system as given in [19]. In the current design, the higher GTF fan weight of 723kg compared to the 410kg of the baseline fan is overcompensated by a smaller core and lighter nacelle configuration. The heaviest engine concept is the CROR engine with a predicted mass of 4097kg. Its two shaft core engine is comprised of a five stage low pressure compressor (LPC), a five stage HPC, and a single stage HPT and intermediate pressure turbine (IPT) respectively. The propulsion unit of the CROR engine consists of a three stage LPT which is connected to the counter rotating propellers by a gearbox of transmission ratio 9.5. Although core and nacelle of the CROR are lighter than for the competing designs, the excessive weight of the propulsion unit outweighs their savings.

It can be seen that the resulting overall pressure ratio of the GTF is about 8% higher than for the CROR. This observation is related to the inevitably smaller core size of the open rotor engine, since higher CROR overall pressure ratios have been prevented by the assumed blade height constraint of the last high pressure compressor stage. In contrast, the OPR of the GTF was practically limited by performance penalties from increased turbine loadings and cooling air requirements only. A way to further increase the overall pressure ratio of the open rotor engine might be the application of axial-radial high pressure compressors, which should be addressed in future studies. Figure 1 compares the turbine entry temperatures (TET) of the GTF and

CROR engines at the design points in relation to temperatures occurring in the baseline model. It is evident that the increase of maximum TET which occurs during the EOF condition is rather small for both novel engines. This can be attributed to the higher thrust lapse rates of the high bypass ratio concepts with altitude. Caused by the same principle, a significant increase in cruise and top of climb TET can be observed. Whereas the baseline engine shows a temperature difference of approximately 260K between EOF and CR condition, the CROR engine exhibits a delta of only 90K. The lower temperature deviations between take-off and cruise may reduce thermal fatigue of the hot end components. However, the higher overall temperature levels might expose the high pressure turbine to increased creep.

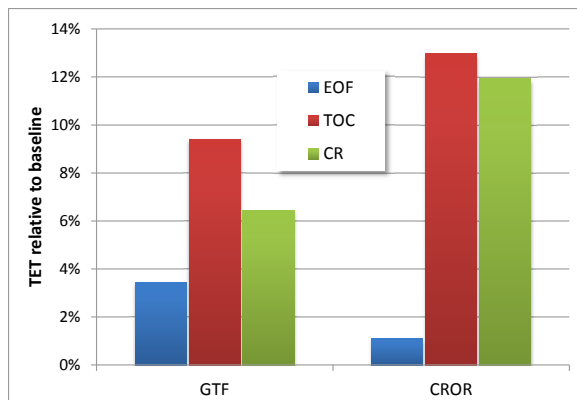


**Figure 1: GTF and CROR relative turbine entry temperatures at mission design points compared to baseline engine.**

As would be expected, a large difference in bypass ratio can be observed between the three models. The cruise BPR of the CROR is roughly seven times larger than that of the GTF engine resulting in a propulsive efficiency advantage. Figure 2 compares the uninstalled SFC improvements of both novel concepts to the thrust specific fuel consumption of the baseline engine. It can be seen that the CROR engine is predicted to cut uninstalled cruise SFC by 36% relative to

baseline. The advanced GTF shows a SFC reduction potential of 20%, which would be another four to five percent improvement compared to the claimed figures of the upcoming PW1100G geared turbofan engine [20]. Although the predicted GTF-SFC should be regarded as a significant efficiency improvement, forthcoming limits of the conventionally installed GTF concept in respect to a further increase of the propulsive efficiency are indicated.

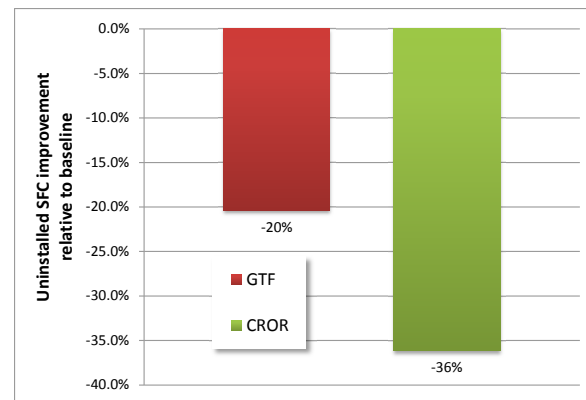


**Figure 2: GTF and CROR uninstalled cruise SFC reduction compared to baseline engine.**

Main restrictions to GTF bypass ratio enhancements are nacelle drag and system weight penalties due to increased fan diameters. Fan weight reduction based on enhanced application of composite materials, reduced core size as well as shorter and lighter nacelles will surely contribute to further efficiency improvements. However, the potential is expected to be in the lower single digit range, as figure 3 suggests. Here the previously optimized GTF engine was taken as reference. The bypass ratio parameter was varied from 12.2 up to 25. Simultaneously the fan pressure ratio was automatically iterated to guarantee optimal extraction ratios. Overall pressure ratio as well as turbine entry temperature were kept constant at 46.9 and 1509K respectively. It can be seen that even by a drastic increase of the bypass ratio to 25, the uninstalled SFC would only improve by less than

4%. At the same time, however, the fan diameter grows by almost 40%. Since fan and nacelle weight as well as nacelle wetted area increase super-proportionally with fan diameter, the efficiency gains are likely to be consumed by installation effects.

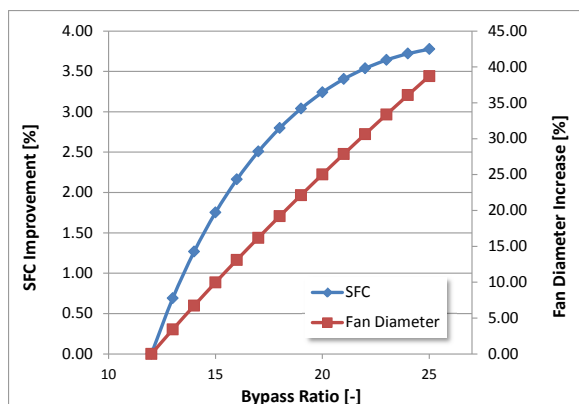


**Figure 3: GTF uninstalled cruise SFC improvement and fan diameter increase for varying bypass ratios.**

Advanced engine installation technologies such as embedded engines seem to be necessary to push the turbofan limitations considerably further.

### The aircraft model

To assess the efficiency potential of both novel engine concepts on flight mission level, DLR's aircraft performance tool VarMission [5] has been used. VarMission aircraft models are represented by characteristic aircraft weights (operational empty weight, maximum take-off weight etc.) and Mach-number-dependent lift-to-drag characteristics for different aircraft configurations. Generic aircraft are simulated by the software that resemble real aircraft types. For the present study, a narrow body aircraft resembling a V2500 powered Airbus A320 was investigated. Both novel engine concepts were considered as exchange engines to the V2500. The following assumptions/modifications were made for the re-engining process:

- Maximum take-off weight (MTOW) and maximum fuel capacity (MFC) of the aircraft were kept constant for all aircraft-engine combinations.
- Differences in engine weight as described above influence the aircraft's operating empty weight (OEW). Assuming that maximum zero fuel weight (MZFW) remains unchanged, maximum payload capacity (MPL) is also affected by changes in engine weight.
- As described earlier, engine-specific and Mach-number-dependent modifications to the aircraft's lift-to-drag characteristics have been applied in order to account for increased drag by larger engines.

It should be noted that except for engine weight deltas, no additional weight penalties are considered, which account e.g. for additional requirements regarding cabin noise insulation for an aft mounted open rotor. Future work needs to be performed to quantify such aspects.

### Flight mission analysis

Using the above aircraft models, a flight mission can be simulated as a sequence of flight segments, which include:

- Taxi-Out and Taxi-In with engines operating at idle thrust.
- Climb at maximum climb thrust and constant calibrated airspeed with an acceleration phase on flight level 100. Further climb at constant Mach number after reaching the transition altitude.
- Constant Mach number Cruise at constant flight level, with or without step climbs.
- Descent at constant Mach number (above transition altitude) and at constant airspeed (below TA) with a deceleration before reaching flight level 100.

For the current study, departure and approach segments are simulated on the basis of the so-called modified ATA departure and low-drag-low-power approach procedures. Typical reserve fuel policies are assumed considering 5% of the trip fuel as contingency, flight to an alternate airport at a distance of 200 nautical miles and 30 minutes holding at low altitude. Given the above mission rules, the payload-range-diagram of the reference aircraft can be computed and is shown in figure 4.

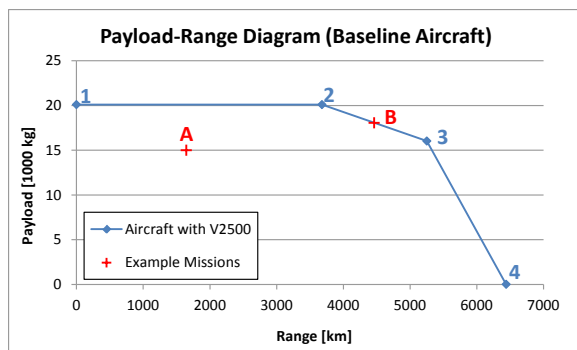


**Figure 4: Payload-Range diagram of baseline aircraft and example flight missions.**

Two different flight missions were simulated for each aircraft-engine configuration in order to assess the fuel efficiency impact of the novel engine concepts. Mission A was selected as a typical flight for the investigated type of aircraft. The mission distance is 1650km, which roughly corresponds to a trip from Berlin Schönefeld (SXF) to Palma de Mallorca (PMI). The cruise altitude is kept constant at flight level 350; climb and cruise Mach numbers are set to Mach 0.78. A payload of 15000kg is assumed for this mission, corresponding e.g. to 150 passengers at 100kg per PAX (including luggage). Example Mission B corresponds to the assumed design mission of the generic reference aircraft, situated between the characteristic point 2 and 3 of the aircraft's payload-range diagram shown in figure 4. For this flight, a payload of 18063kg is transported over a distance of 4465km. Cruise

altitudes were set to flight levels 350-370, including a mid-cruise step climb (see Figure 5). A constant cruise Mach number of M0.78 is assumed for this flight.

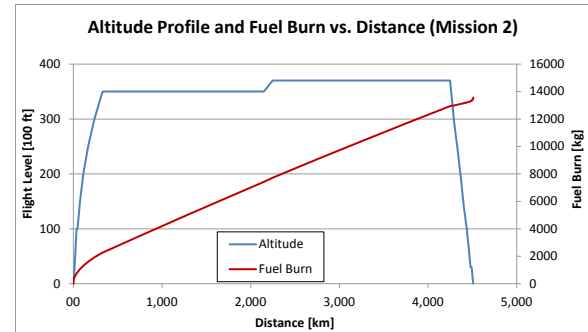


**Figure 5: Altitude profile and fuel burn vs. distance for example mission 2 (baseline aircraft).**

Table 6 summarizes the results of the flight mission simulations. Both re-engined aircraft configurations show significant fuel consumption benefits over the aircraft equipped with the baseline engine. For mission B over 4465km, the GTF-configuration is able to reduce fuel consumption by 19.4% relative to baseline. For the same mission the CROR-configuration cuts fuel burn by 30.2% which corresponds to a relative improvement of 13.4% compared to the advanced geared turbofan. As may be expected, the block fuel benefit of both conceptual engines is smaller for shorter flight distances. For mission A, the advantages of the GTF- and CROR-configurations over the baseline are 18.8% and 28.8% respectively.

| Engine | Parameter     | Unit | Mission |       |
|--------|---------------|------|---------|-------|
|        |               |      | A       | B     |
| All    | Distance      | [km] | 1650    | 4465  |
|        | Payload       | [kg] | 15000   | 18063 |
| V2500  | TOW           | [kg] | 65666   | 77000 |
|        | Fuel Burn     | [kg] | 5657    | 13565 |
| GTF    | TOW           | [kg] | 63543   | 73298 |
|        | Fuel Burn     | [kg] | 4592    | 10929 |
|        | $\Delta$ Fuel | [%]  | -18.8   | -19.4 |
| CROR   | TOW           | [kg] | 64556   | 73328 |
|        | Fuel Burn     | [kg] | 4052    | 9462  |
|        | $\Delta$ Fuel | [%]  | -28.8   | -30.2 |

**Table 6: Flight mission results for all three aircraft-engine configurations.**



Taking into account the more advanced technology level assumed for the conceptual engines, the GTF-benefits on mission level compare well to the 15% advantage claimed by Airbus and Pratt & Whitney for the A320NEO compared to its predecessor. The relative CROR-advantage over the geared turbofan is 11.8%.

### Influence on payload-range performance

Figure 6 shows the influence of the novel engine concepts on the payload-range performance of the aircraft. Given the aforementioned modeling assumptions, the increased weight of the open rotor engine results in a reduction of the aircraft's maximum structural payload (MPL) by 1390kg, whereas a (minor) increase of the MPL can be observed for the GTF-powered version. As can be seen in Figure 6, the improved fuel efficiency of the new concepts compared to the baseline engine translates into increased maximum ranges in all points of the PL-R-diagrams. At MPL, an additional range of 1190km (640 NM) can be observed for the GTF-powered aircraft, with even higher deltas in points 3 and 4 of the diagram. At high payloads, the efficiency advantage of the CROR does not translate into a notably higher range compared to the GTF, due to its higher weight.

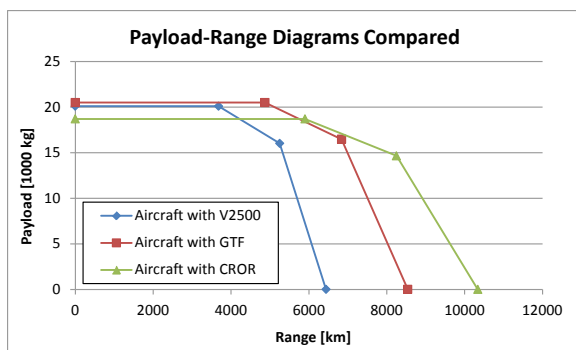


**Figure 6: Influence of re-engining on aircraft payload-range performance.**

It should be noted that for the current assessment, both conceptual engines are optimized and compared

for a cruise Mach number of M0.78. A higher advantage of the CROR concept in terms of fuel efficiency and range can be expected if lower cruise speeds were accepted and used for engine optimization.

### Conclusions and Outlook

In the present paper a comparison in regard to fuel efficiency between an advanced geared turbofan and a counter rotating open rotor engine available in 2025 was carried out. Both engine concepts have been designed and optimized on basis of the same assumed technology level and were used to re-engine a baseline generic 150PAX civil airliner. Although the counter rotating open rotor engine was predicted to have a weight penalty of approximately 28% in comparison to the advanced GTF, its benefits in terms of propulsive efficiency outweighed these problems. Mission analysis showed a fuel burn advantage of the CROR-configuration between 12-13% over the advanced GTF, depending on the mission profile under consideration. Compared to a 1990s baseline configuration, the fuel burn advantages are predicted to lie in the range of 29-30%. However, assumptions and modeling methods of the present study in respect to engine installation effects need to be further improved in order to assure the aforementioned benefits. Taking the claimed fuel burn improvements of the upcoming PW1000G and LEAP-X engine generation into account, the open rotor seems to have the potential to offer another double digit efficiency improvement for the 2025 engine generation. Here, the investigated advanced GTF drops behind because of the drag and weight penalties of conventional nacelle installations. Advanced engine-airframe integration, such as embedded engines, may help to partially circumvent the turbofan limitations. As has been observed, the high bypass ratios of both concepts lead to small core sizes

and increased cruise and top of climb operating temperatures. To respond to this development, technology modifications in order to increase the specific power of the core need to be addressed in future studies.

### References

- [1] Kurzke, J., *Achieving maximum thermal efficiency with the simple gas turbine cycle*, 9th CEAS European Propulsion Forum, 15-17 October 2003, Roma, Italy
- [2] Dewanji, D., Rao, G., van Buijtenen, *Feasibility Study of Some Novel Concepts for High Bypass Ratio Turbofan Engines*, ASME Turbo Expo 2009, June 8-12, Orlando, GT2009-59166
- [3] Kurzke, J., *Fundamental differences between conventional and geared turbofans*, ASME GT2009-59745
- [4] Becker, R.-G., Wolters, F., Nauroz, M., Otten, T., *Development of a gas turbine performance code and its application to preliminary engine design*, German Aerospace Congress DGLRK, Bremen, Germany, September 2011
- [5] Schaefer, M., *Development of a forecast model for global air traffic emissions*, DLR Forschungsbericht 2012-08, Köln, 2012
- [6] ModelCenter™ Website, <http://www.phoenix-int.com/software/phx-modelcenter.php>, April 2013
- [7] ICAO Aircraft Engine Emissions Databank Website, <http://easa.europa.eu/environment/edb/aircraft-engine-emissions.php>, April 2013
- [8] Schnell, R., Ebel, P.-B., Becker, R.-G., Schoenweitz, D., *Performance Analysis of the Integrated V2527-Engine Fan at Ground Operation*, ODAS, 2013
- [9] Otten, T., Becker, R., Plohr, M., Döpelheuer, A., *Energy Efficient Engine Concepts*, NATO AVT-Workshop on Energy Efficient Technologies and Concepts of Operation, October 2012, Lisbon, Portugal
- [10] Grieb, H., *Projektierung von Turboflugtriebwerken*, Birkhauser Verlag, 2004
- [11] Larsson, L., Avellán, R., Grönstedt, T., *Mission optimization of the geared turbofan engine*, ISABE, Gothenburg, 2011, ISABE-2011-1314
- [12] Berton, J., Gynn, M., *Multi-Objective Optimization of a Turbofan for an Advanced, Single-Aisle Transport*, NASA/TM-2012-217428
- [13] Horlock, J., Watson, D., Jones, T., *Limitations on gas turbine performance imposed by large turbine cooling flows*, Journal of engineering for gas turbines and power, 2001, vol. 123, pp. 487-494
- [14] Sagerser, D., Lieblein, S., Krebs, R., *Empirical expressions for estimating length and weight of axial-flow components of VTOL powerplant*, NASA-TM-X-2406, 1971
- [15] Jackson, A., *Optimisation of aero and industrial gas turbine design for the environment*, PhD Thesis, Cranfield University, UK, 2009
- [16] Hendricks, E., Ton, M., *Performance and Weight Estimates for an Advanced Open Rotor Engine*, NASA/TM-2012-217710
- [17] Weisbrich, A. L., Godston, J., Bradley, E.S., *Technology and benefits of high speed aircraft counter rotation propellers*, NASA CR-168253, 1982
- [18] D.P. Raymer. *Aircraft Design: A Conceptual Approach*. Second Edition; ISBN 0-930403-51-7, 1992
- [19] Daly, M. (ed.), Gunston, B. (ed.), *Jane's Aero-Engines*, Issue Twenty-seven, IHS Global Limited, March 2010
- [20] Pratt&Whitney PW1000G Website, [http://www.purepowerengine.com/fuel\\_burn.html](http://www.purepowerengine.com/fuel_burn.html), April 2013